Fragment-Based Drug Design: How Big Is Too Big?

Philip J. Hajduk†

Pharmaceutical Discovery Division, Abbott Laboratories, R46Y, AP-10, 100 Abbott Park Road, Abbott Park, Illinois 60064

Received May 1, 2006

Much has been discussed about the proper physicochemical properties (e.g., molecular weight, hydrophobicity, etc.) that should be considered when utilizing fragment leads in drug design. However, little has been reported as to what emphasis, if any, should be placed on the potency of the resulting fragment leads. In this report, a retrospective analysis of 18 highly optimized inhibitors is described in which the compounds were systematically deconstructed until the minimal binding elements could be identified. An analysis of the potency changes that were observed as the leads were reduced in size indicate that a nearly linear relationship exists between molecular weight and binding affinity over the entire range of sizes and potencies represented in the dataset. On the basis of these observations, prediction maps can be constructed that enable critical and quantitative assessments of the process of lead identification and optimization. These data place well-defined limits on the ideal size and potency of fragment leads that are being considered for use in fragment-based drug design.

Introduction

Fragment-based drug design has become an important and powerful tool for the discovery and optimization of new drug leads.[1−3] Since the first description of SAR by NMR in 1996,[4] there have been numerous examples of using both NMR spectroscopy as well as X-ray crystallography to identify low molecular weight (MW ≤ 250), weakly active ligands (K_D ∼ 100−1000 μM) and then translate these compounds into low nanomolar inhibitors using a variety of design strategies.[5−9] In its essence, fragment-based drug design attempts to describe high-affinity ligands in terms of the molecular pieces that comprise a composite inhibitor. Thus, the design and optimization of the ultimate lead compound is carried out by identifying and optimizing the individual fragments, followed by synthetic linking or merging to produce the high-affinity drug lead. Over the past decade, much has been learned about working with and manipulating fragment leads,[10] including library development and design,[11,12] screening methods,[6,13] structure-based design strategies,[14−16] and the energetics of fragment-linking.[17] It is generally accepted that fragment leads need to be smaller (MW < ∼250 Da) and less lipophilic (ClogP < ∼3) than conventional HTS leads to be successfully progressed into clinical candidates that possess good physicochemical properties. However, there is still no clear consensus as to what constitutes an acceptable fragment lead in terms of potency *with respect to* these properties. For example, what is the probability that a fragment lead with a molecular weight (MW) of 250 Da and a K_D value of 1 mM will yield a low nM inhibitor that is rule-of-five compliant?[18] While much has been discussed about the value of using binding efficiency indices (BEIs) to identify leads that exhibit the greatest potency relative to their size,[19,20] what happens to the binding efficiency as fragment leads are progressed to higher MW inhibitors? Answers to these questions can significantly affect the choice of fragment leads as well as enable a critical assessment of the fragment and lead optimization process.

To address these questions, a retrospective analysis was performed on 18 highly optimized drug leads for 15 different protein targets from our internal drug discovery programs. The results allow for a rigorous assessment of fragment leads and of the lead optimization process in general. In addition, the results challenge some traditional notions of molecular recognition, and provide strong empirical support for the success of fragment-based screening approaches in general.

Results

In this study, 18 drug leads from 15 different internal discovery programs (11β-HSD-1, Akt-1, Bcl-xL, CHK-1, DPP-4, HCV polymerase, Jnk-1, KDR, MetAP-2, PARP, PTP-1B, Survivin, MMP-3, H3, and VR1) were systematically reduced in size (tracking the potency of all intermediate compounds) until the lowest molecular weight compound with a reported potency value was identified. These drug leads were specifically chosen as they were considered to be the final product(s) of extensive synthetic optimization programs, thus representing the best achievable balance between potency, safety, and bioavailability. In fact, eight of these compounds were approved for preclinical development, an additional eight compounds were used in advanced in vivo evaluation studies, and the final two compounds exhibited the best in vitro profiles at the time the projects were terminated (see Supporting Information Table S1 for available information). It is also important to stress that the deconstruction process included only those molecules whose chemical structure was either identical to or most closely related to that which existed in the final inhibitor. Thus, the chemical structure of the final inhibitor dictated the compounds that were identified in the deconvolution process. An example of this deconstruction process is depicted in Figure 1A for the Bcl-xL inhibitor ABT-737 (additional examples are given in the Supporting Information Figure S1).[21] In this example, various groups on ABT-737 (MW = 813, K_I = 0.5 nM, pK_D = 9.3) were sequentially removed or appropriately transformed to yield the simple biaryl acylsulfonamide **6** (MW = 293, K_D = 320 μM, pK_D = 3.5).[22] What is striking about these data is that there is a remarkably linear relationship between molecular weight and binding affinity. As shown in Figure 1B for Bcl-xL, the relationship between pK_D and MW is almost perfectly linear (R^2 = 0.98), while the binding efficiency index (defined as the pK_D divided by the MW in kDa)[20] remains constant at a value

† To whom correspondence should be addressed. Phone: (847) 937-0368. Fax: (847) 938-2478. E-mail: philip.hajduk@abbott.com.

10.1021/jm060511h CCC: $33.50
Published on Web 11/09/2006

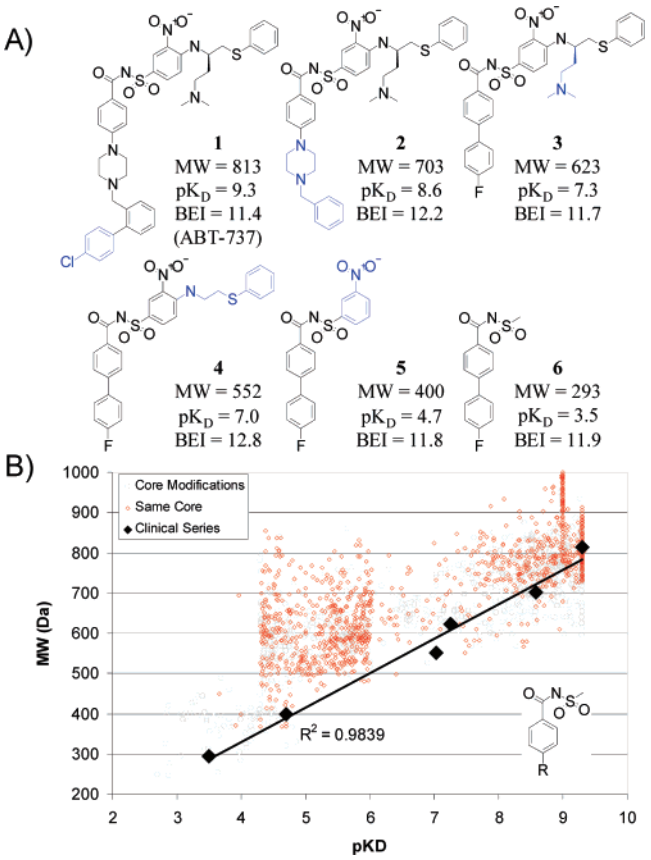

Figure 1. (A) The process of deconstructing an optimized inhibitor of Bcl-xL by sequentially removing or appropriately transforming specific groups (highlighted in blue) until a minimal binding element could be identified. The MW, pK_D (defined as the negative base-10 logarithm of the K_D value expressed in molar units), and BEI (defined as the pK_D divided by the MW in kDa) values are given for each compound. (B) pK_D values for the six Bcl-xL compounds depicted in (A) plotted against MW (black diamonds, left *y*-axis) or binding efficiency (red squares, right *y*-axis). Also shown are pK_D and MW data for >2300 compounds synthesized throughout the course of the project that contain the core shown in the lower right. Compounds with R = 4-phenyl or 4-*N*-piperizinyl (the cores in the initial fragment **6** and final clinical candidate **6**) are shown as red circles. Compounds with alternative cores are shown as gray diamonds.

of ~12. Also shown in Figure 1B are potency and MW data for more than 2300 structurally related compounds that were prepared during the course of the Bcl-xL project (depicted as red circles and gray diamonds). As will be discussed in more detail below, the six concept compounds exhibit higher binding efficiency indices than 94% of all compounds prepared for the project.

A similar process was followed for the additional 17 lead inhibitors. On average, approximately 4.1 conceptual steps were required to progress from fragment lead to optimized inhibitor, resulting in a total of 73 compounds for all 18 series. For the examples given here, the average MW decreased from 463 to 224 Da when progressing from final compound to fragment, while the average pK_D value decreased from 8.3 (K_D ~ 5 nM) to 4.7 (K_D ~ 20 μM). As shown in Figure 2A, all series exhibited an essentially linear relationship between potency and molecular weight. In fact, these relationships are nearly colinear, with an average value for the slope of 64 ± 18 overall series. These data imply that, along the path of ideal optimization, an increase of 1 pK_D unit can be expected for every 64 mass units added to the compound. Related to the constancy in the slope, a similar constancy in the binding efficiency was maintained

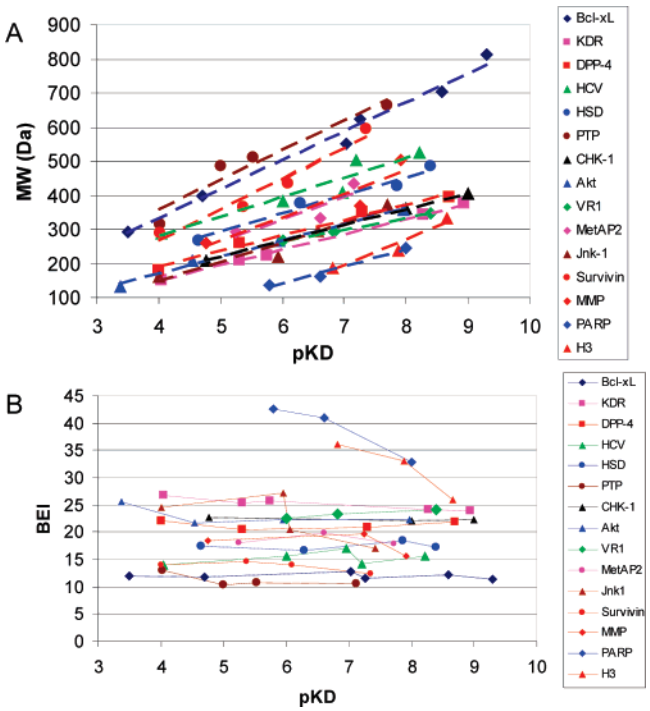

Figure 2. (A) Plots of pK_D values vs MW for compounds identified in the deconstruction of leads for all 15 targets used in the analysis. Two additional chemical series for DPP-4 and one additional chemical series for CHK-1 are not shown for clarity. Best-fit linear trends are shown in dashed lines for each series and colored according to the legend. (B) Plots of pK_D values vs BEI for all 15 targets used in the analysis. Two additional chemical series for DPP-4 and one additional chemical series for CHK-1 are not shown for clarity.

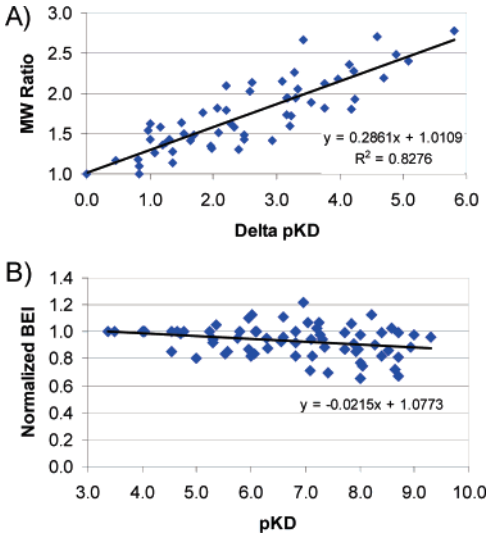

Figure 3. (A) Plot of the change in pK_D for the 73 compounds used in the analysis relative to the MW ratio relative to the minimal fragment lead for each series. A best-fit linear trend is shown. (B) Plot of the pK_D value vs the normalized BEI value (normalized to the smallest fragment in the chemical series) for all 73 compounds used in this analysis. A best-fit linear trend is shown

in progressing from fragment to drug lead for most of the other series as well (see Figure 2B), although several series exhibited rather significant decreases (most noticeably for PARP and H3). Given the nearly parallel correlations observed between potency and either molecular weight or binding efficiency, the data for all of these sets of compounds can be normalized relative to the smallest compound in each series. As shown in Figure 3A, there is a remarkably linear relationship between the change in

pK_D (ΔpK_D) and the fractional change in molecular weight. Similarly, as shown in Figure 3B, the binding efficiency for all of these series exhibits only a moderate overall decrease as potency increases, maintaining an average value of 84 ($\pm$10)% of the original value, regardless of the change in pK_D.

Discussion

One of the more interesting conclusions that can be drawn from these data is that, while moving along an ideal path from optimized fragment to optimized drug lead, every mass unit that is added to the initial fragment contributes equally and proportionally to the binding affinity. This has several potentially significant implications for fragment-based drug design. First, the constancy in the binding efficiency can be used as a quantitative measure of effective fragment elaboration. For example, as the size of the fragment is increased through synthetic means, a drop in the BEI of more than 10% is likely an indication that either the site or the nature of the modification is not ideal, even if modest gains in potency are achieved. This should encourage a more extensive exploration of the chemical space around the site of modification or abandonment of the modification in favor of more fruitful avenues, avoiding the common trap of pursuing potency gains at the (unnecessary) cost of excess mass. Second, these data highlight the importance of beginning with the most efficient fragment lead, regardless of absolute potency or molecular weight. Because efficiency (or inefficiency) remains constant throughout lead optimization, beginning with a suboptimal fragment lead can frustrate subsequent optimization efforts, especially when trying to balance multiple properties such as solubility, permeability, and stability. This is especially true as the current analysis highlights the low probability of actually increasing binding efficiency simply by adding substituents to an otherwise invariant core. This is supported by the fact that the six "concept" compounds shown in Figure 1 stay at or near the front of the pK_D − MW distribution (e.g., exhibit the highest potency for the least mass) until extremely high potency is achieved (pK_D > 8). Compounds 1−6 exhibit an average binding efficiency index of 12.0 $\pm$ 0.4, which is greater than 94% of all compounds made on the project, and only 3% of all compounds synthesized exhibit a BEI greater than 13 (representing an increase in average BEI of 8.3%). Significantly, the majority of these more efficient compounds (~79%) contain a modified core (distinct from either the biphenyl or the phenyl-piperizine cores, see Figure 4), highlighting the importance of exploring core modifications (e.g., heteroatom replacements, ring changes, and other "lead-hopping" exercises) in the context of the fragment lead until the highest potency per mass unit is realized.

One can also use these data to predict the expected size of a final, optimized inhibitor based on the characteristics of the fragment lead itself, assuming that the fragment core remains unchanged and that additional substituents are simply added to the molecule. The linear relationship between ΔpK_D and MW ratio (Figure 3A) can be used to calculate the change in mass necessary for a desired change in affinity. Simple estimates from the plot indicate that to achieve potency gains of 3 or 6 log units, the mass of the compound would need to be increased by approximately a factor of 1.9 or 2.9, respectively. For example, if one started with a fragment lead of 250 Da and a binding affinity of 1 mM (pK_D = 3), then achieving a compound with a K_D value of 1 nM (a gain of 6 in pK_D) would require a compound with a mass of 750 $\pm$ 45 Da. This observed linear relationship between potency and mass can be used to construct prediction maps that use the MW and pK_D values of the initial

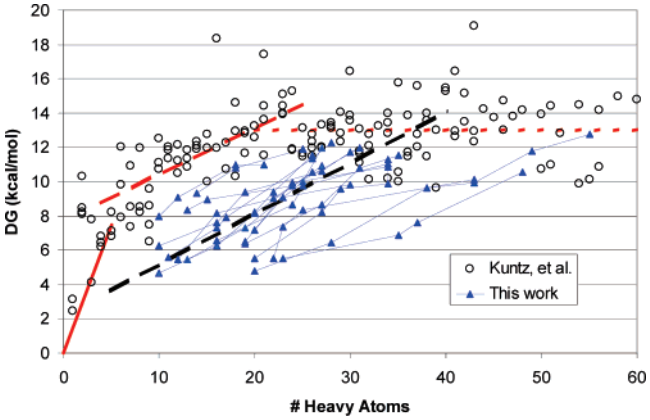

Figure 4. Plots of the number of heavy atoms per compound against the calculated free energy of binding ($\Delta G = -RT \ln K_D$ at 300 K)[22] for the compounds described in the current work (blue triangles) and to a set of widely diverse ligands reported by Kuntz et al. (black circles).[24] For the compounds in the current work (blue triangles), each chemical series is connected by a solid blue line, although no attempt is made to discriminate between different series. Kuntz et al. observed a rapid initial rise of ~1.5 kcal/mol per heavy atom (denoted by the solid red line), with a plateau of approximately −0.0002 kcal/mol per atom beyond 25 atoms (denoted by the short-dashed red line). Each of the series in the current work increases in binding energy at a relatively constant rate of 0.3 kcal/mol per atom. The dashed black line denotes the average overall series in this work. This average slope is very close to that observed in the data set from Kuntz et al., if only the ligands with 5−25 atoms are used (long-dashed red line, slope = 0.27 kcal/mol per atom).

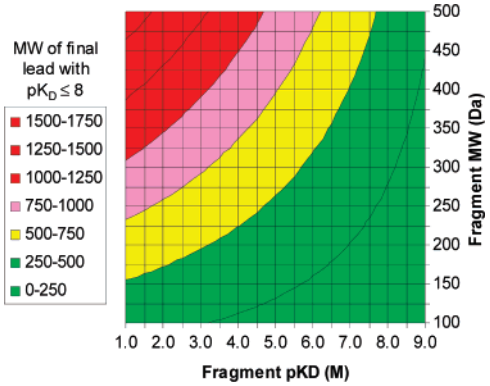

Figure 5. Prediction plot of the expected molecular weight of a final optimized inhibitor with a potency of ≤10 nM when starting with optimized leads of various potency and MW values. This graph was based on the linear trend observed in Figure 3A.

fragment to estimate the molecular weight of a drug candidate of defined potency. An example of this is shown in Figure 5 for achieving a potency value of less than or equal to 10 nM. The green areas of this graph demarcate regions where the mass and potency of the initial fragments can be optimized to final nM compounds whose mass is predicted to be less than 500 Da. In this case, a 1 mM fragment lead (pK_D = 3) would need to have a MW less than 200 Da to remain rule-of-five compliant after optimization. Depending on the acceptable MW for a given therapeutic indication, this graph can be used to abandon particular fragments or even entire screening sets if they do not fall within or near the desired region. For example, a rigorous requirement for rule-of-five compliance would dictate abandonment of all fragment leads with a MW of 250 or greater unless the potency was substantially better than 30 μM.

Previous analyses have examined the process of lead optimization from initial HTS lead to clinical candidate,[23] noting a general increase in size and hydrophobicity. However, conclu-

sions about the correlation between MW and potency changes were not discussed and are likely not applicable as the lead compounds used in the analysis did not represent ideal or near-ideal starting points, but simply the chemical matter derived from the lead identification process. In fact, approximately 44% of the drug-lead pairs used in the analysis by Oprea et al., entailed modifications to the core of the lead molecule to produce the drug, while an additional 20% of the molecules represented leads that were progressed as drugs with no modification (see Supporting Information for ref 23). This is very different from the current retrospective analysis, which is by definition using optimized fragment leads (the structures that ultimately formed the cores of the clinical or preclinical candidates). As a result, the identified low molecular weight structures have all the benefits of the synthetic optimization that went into defining and crafting the optimal substituents. Thus, the predictions derived from the current analysis should ideally be applied only to fragment leads whose structure−activity relationships have been explored to the extent that compounds with the maximal or near-maximal binding efficiency can be used. It is, however, anticipated that these prediction maps can be used in the analysis of hits derived from high-throughput screening, especially if the compounds can be deconstructed to identify the core binding elements that impart the majority of the binding energy. HTS leads that can be deconstructed to fragments that fall within an acceptable range of potency and MW on the prediction map should be prioritized for further optimization. This requires taking a fragment-based view of initial drugs leads, which may necessitate testing the putative fragments at high compound concentrations (100−1000 μM) to effectively evaluate their potential for further optimization.

It is also instructive to compare this fragment analysis to that of Kuntz et al. in their study on the maximal affinity of ligands.[24] This previous work explored the relationship between size and potency for a set of 160 endogenous or highly optimized ligands for different protein targets. As shown in Figure 4, Kuntz et al. observed a rapid increase of ∼1.5 kcal/mol per heavy atom (solid red line in Figure 4), with no net gains in potency beyond 25 heavy atoms (dashed red line in Figure 4). Our results are in good qualitative agreement with those of Kuntz et al., in that all series approach a limit of ∼12 kcal/mol as the molecules are increased in size. Kuntz et al. rationalized that this apparent limit on the maximal affinity of ligands may be due to significant shielding of van der Waals and hydrophobic interactions, such that as the number of ligand atoms increases, the average contribution per atom to the binding energy decreases.[24] However, the results of the current deconstruction analysis suggest that, beyond ∼15 atoms, successful lead optimization yields an approximately constant increase of 0.30 kcal/mol per additional atom (dashed black line in Figure 4), at least until this limit of ∼12 kcal/mol is attained. Interestingly, if only the ligands with 5−25 atoms are used from the data set of Kuntz et al., a slope of 0.27 kcal/mol per atom is obtained (long-dashed red line in Figure 4), very close to the value observed in this work. A value of 0.3 kcal/mol per atom has also been previously suggested to be a minimum binding efficiency for lead selection.[19] This observed monotonic increase in binding energy per additional atom argues against very significant "self-shielding" as the molecules increase in size, even though some losses in potential binding energy can be expected.[25] Instead, these targets are differentiated primarily by the amount of binding energy that can be attained with the initial 10−20 atoms. The fact that certain protein targets yield more free energy of binding per atom for the core binding element (the "fragments" identified in this retrospective analysis) is completely consistent with the notion of assessing protein druggability on the basis of a protein's ability to bind to fragment molecules.[26] In other words, certain protein subsites are simply "hotter" than others,[27,28] but this energetic focal point is spatially restricted to a volume corresponding to ∼10−20 heavy atoms. This differentiation between protein targets is most clearly observed in Figure 2B, where some protein targets appear to be more easily druggable (e.g., kinase inhibitors maintain a binding efficiency of ∼23), while others are more difficult (e.g., protein−protein interaction inhibitors maintain a binding efficiency of ∼12). In fact, the same trends emerge if one looks closely at the list of ligands used by Kuntz et al. For example, ligands of only 11−18 heavy atoms are required for high affinity binding to GPCRs (e.g., cholinergic receptors, adrenergic receptors, etc), while compounds of more than 36 heavy atoms are required to achieve the same potency against HIV protease.[24] This is fully consistent with the notion that certain proteins simply require larger molecules to achieve therapeutically useful binding.

Conclusions

Fragment-based drug design continues to expand and evolve. As our understanding of protein−ligand interactions and molecular recognition increases, our ability to rapidly develop potent and selective inhibitors of therapeutically relevant targets can be dramatically enhanced. The relationships derived here between molecular weight and potency provide intriguing insight into the energetics of ligand binding. Their appropriate use in a drug discovery setting should improve our ability to critically assess the identification and optimization of lead compounds that have high potential for generating new therapeutic agents.

Methods

Lead Deconstruction. For each compound used in this study, single substituents were individually removed and searches of our corporate database were performed to identify potential progenitor compounds with available activity data against the target of interest. Once a progenitor was identified, substituents were individually removed from it and searches for new progenitor compounds were performed. This process was continued until no further compounds could be identified. In a few cases, exact progenitor compounds for certain molecules could not be identified. In these circumstances, minor differences were allowed (e.g., fluorine for hydrogen) or compounds from the actual path of the optimization process were utilized (as illustrated in Figure 1, with the identification of compound **3** as the progenitor of **2** for Bcl-xL). For each target, the exact assay and result type (e.g., IC_{50}, K_I, K_D, etc.) were used for each compound in the series. However, no distinction was made between targets (i.e., the pK_D value reported is the negative base-10 log of the IC_{50}, K_I, or K_D, depending on the particular target).

Acknowledgment. The author would like to thank Drs. Jonathan Greer, Steve Muchmore, and Cele Abad-Zapatero for helpful discussions and critical reading of the manuscript.

Supporting Information Available: Additional examples of inhibitor deconstruction and a table of additional information on the final products of extensive synthetic optimization programs. This material is available free of charge via the Internet at http://pubs.acs.org.

References

(1) Rees, D. C.; Congreve, M.; Murray, C. W.; Carr, R. Fragment-based lead discovery. *Nat. Rev. Drug Discovery* **2004**, *3*, 660−672.
(2) Erlanson, D. A.; McDowell, R. S.; O'Brien, T. Fragment-based drug discovery. *J. Med. Chem.* **2004**, *47*, 1−20.
(3) Zartler, E. R.; Shapiro, M. J. Fragonomics: Fragment-based drug discovery. *Curr. Opin. Chem. Biol.* **2005**, *9*, 366−370.

(4) Shuker, S. B.; Hajduk, P. J.; Meadows, R. P.; Fesik, S. W. Discovering high-affinity ligands for proteins: SAR by NMR. *Science* **1996**, *274*, 1531−1534.
(5) Stockman, B. J.; Dalvit, C. NMR screening techniques in drug discovery and drug design. *Prog. Nucl. Magn. Reson. Spectrosc.* **2002**, *41*, 187−231.
(6) Meyer, B.; Peters, T. NMR spectroscopy techniques for screening and identifying ligand binding to receptors. *Angew. Chem., Int. Ed.* **2003**, *42*, 864−890.
(7) Carr, R.; Jhoti, H. Structure-based screening of low-affinity compounds. *Drug Discovery Today* **2002**, *7*, 522−527.
(8) Hartshorn, M. J.; Murray, C. W.; Cleasby, A.; Frederickson, M.; Tickle, I. J.; et al. Fragment-based lead discovery using X-ray crystallography. *J. Med. Chem.* **2005**, *48*, 403−413.
(9) Hajduk, P. J. Applications of receptor-based NMR screening in drug discovery. *Mod. Magn. Reson.* **2006**, *in press*.
(10) Huth, J. R.; Sun, C.; Hajduk, P. J. Utilization of NMR-derived fragment leads in drug design. *Methods Enzymol.* **2005**, *394*, 549−572.
(11) Lepre, C. A. Library Design for NMR-Based Screening. *Drug Discovery Today* **2001**, *6*, 133−140.
(12) Baurin, N.; Aboul-Ela, F.; Barril, X.; Davis, B.; Drysdale, M.; et al. Design and characterization of libraries of molecular fragments for use in NMR screening against protein targets. *J. Chem. Inf. Comput. Sci.* **2004**, *44*, 2157−2166.
(13) Pellecchia, M. Solution nuclear magnetic resonance spectroscopy techniques for probing intermolecular interactions. *Chem. Biol.* **2005**, *12*, 961−971.
(14) Dean, P. M.; Lloyd, D. G.; Todorov, N. P. De novo drug design: Integration of structure-based and ligand-based methods. *Curr. Opin. Drug Discov. Devel.* **2004**, *7*, 347−353.
(15) Verdonk, M. L.; Hartshorn, M. J. Structure-guided fragment screening for lead discovery. *Curr. Opin. Drug Discovery Dev.* **2004**, *7*, 404−410.
(16) Kitchen, D. B.; Decornez, H.; Furr, J. R.; Bajorath, J. Docking and scoring in virtual screening for drug discovery: Methods and applications. *Nat. Rev. Drug Discovery* **2004**, *3*, 935−949.
(17) Hajduk, P. J. SAR by NMR: An analysis of potency gains realized through fragment-linking and fragment-elaboration strategies for lead generation. *Methods Princ. Med. Chem.* **2006**, *34*, 181−192.
(18) Lipinski, C. A. Drug-like properties and the causes of poor solubility and poor permeability. *J. Pharmacol. Toxicol. Methods* **2000**, *44*, 235−249.
(19) Hopkins, L. A.; Groom, C. R.; Alex, A. Ligand efficiency: A useful metric for lead selection. *Drug Discovery Today* **2004**, *9*, 430−431.
(20) Abad-Zapatero, C.; Metz, J. T. Ligand efficiency indices as guideposts for drug discovery. *Drug Discovery Today* **2005**, *10*, 464−469.
(21) Oltersdorf, T.; Elmore, S. W.; Shoemaker, A. R.; Armstrong, R. C.; Augeri, D. J.; et al. An inhibitor of Bcl-2 family proteins induces regression of solid tumours. *Nature* **2005**, *435*, 677−681.
(22) For the purposes of this analysis, no attempt was made to differentiate between K_D, K_I, and IC_{50} values. However, the same result type from the same assay was used within each chemical series.
(23) Oprea, T. I.; Davis, A. M.; Teague, S. J.; Leeson, P. D. Is there a difference between leads and drugs? A historical perspective. *J. Chem. Inf. Comput. Sci.* **2001**, *41*, 1308−1315.
(24) Kuntz, I. D.; Chen, K.; Sharp, K. A.; Kollman, P. A. The maximal affinity of ligands. *Proc. Natl. Acad. Sci. U.S.A.* **1999**, *96*, 9997−10002.
(25) Li, Y.; Huang, Y.; Swaminathan, C. P.; Smith-Gill, S. J.; Mariuzza, R. A. Magnitude of the hydrophobic effect at central versus peripheral sites in protein-protein interfaces. *Structure* **2005**, *13*, 297−307.
(26) Hajduk, P. J.; Huth, J. R.; Fesik, S. W. Druggability indices for protein targets derived from NMR-based screening data. *J. Med. Chem.* **2005**, *48*, 2518−2525.
(27) DeLano, W. L. Unraveling hot spots in binding interfaces: Progress and challenges. *Curr. Opin. Struct. Biol.* **2002**, *12*, 14−20.
(28) Kortemme, T.; Baker, D. A simple physical model for binding energy hot spots in protein-protein complexes. *Proc. Natl. Acad. Sci. U.S.A.* **2002**, *99*, 14116−14121.

JM060511H